

Electronic Supplementary Information

Halogen and solvent effects induced structural transformation and isostructural luminescence regulation in copper-based hybrid halides

Lin Yang,^{‡a} Yani Li,^{‡a} Xia Liu,^a Bohan Li^a and Yan Xu^{*ab}

^a Department of Chemistry, College of Sciences, Northeastern University, Shenyang, Liaoning 110819, China

^b Foshan Graduate School of Innovation, Northeastern University, Foshan, Guangdong, 528311, China

***Corresponding Authors:**

xuyan@mail.neu.edu.cn (Yan Xu)

Experimental Section:

Materials

Cuprous bromide (CuBr, 99%, Aladdin), Cuprous iodide (CuI, 99%, Aladdin), Isopropyltriphenylphosphonium bromide ($[\text{C}_{21}\text{H}_{22}\text{P}]\text{Br}$, $\geq 98\%$, Aladdin), Isopropyltriphenylphosphonium iodide ($[\text{C}_{21}\text{H}_{22}\text{P}]\text{I}$, $\geq 98\%$, Aladdin), Hypophosphorous acid (H_3PO_2 , 50% wt. in H_2O , Aladdin), Sodium iodide (NaI , $\geq 99.5\%$, Aladdin), Methanol (99.5%, General-Reagent), Ethanol (99.7%, General-Reagent), Acetonitrile (99.8%, $\text{H}_2\text{O} \leq 0.001\%$), Acetone (99.7%, Sinopharm). All chemicals were used without further purification.

Syntheses

Synthesis of $(C_{21}H_{22}P)_2(CuBr_3) \cdot H_2O$ (L1). CuBr (0.1 mmol), $[C_{21}H_{22}P]Br$ (0.3 mmol) and H_3PO_2 (0.5 mL) were dissolved in acetone (5 mL). Stirring until the solution is clear and transparent, leaving it at room temperature. Then, L1 crystals were gradually precipitated and collected as the solvent evaporated.

Synthesis of $(C_{21}H_{22}P)_2(CuI_3) \cdot 0.62H_2O$ (L2). CuI (0.1 mmol), $[C_{21}H_{22}P]I$ (0.3 mmol) and H_3PO_2 (0.5 mL) were dissolved in acetone (25 mL). Stirring until the solution is clear and transparent, leaving it at room temperature. Then, L2 crystals were gradually precipitated and collected as the solvent evaporated.

Synthesis of $(C_{21}H_{22}P)(Cu_2I_4)_{0.5}$ (P1). CuI (0.1 mmol), $[C_{21}H_{22}P]I$ (0.1 mmol) and H_3PO_2 (0.5 mL) were dissolved in acetonitrile (10 mL). Stirring until the solution is clear and transparent, leaving it at room temperature. Then, P1 crystals were gradually precipitated and collected as the solvent evaporated.

Synthesis of $(C_{21}H_{22}P)(Cu_2I_4)_{0.5}$ (P2). CuI (0.1 mmol), $[C_{21}H_{22}P]I$ (0.2 mmol) and H_3PO_2 (0.5 mL) were dissolved in acetonitrile (10 mL). Stirring until the solution is clear and transparent, leaving it at room temperature. Then, P2 crystals were gradually precipitated and collected as the solvent evaporated.

Synthesis of $(C_{21}H_{22}P)(Cu_2I_4)_{0.5}$ (P3). CuI (0.1 mmol), $[C_{21}H_{22}P]I$ (0.3 mmol) and H_3PO_2 (0.5 mL) were dissolved in acetonitrile (5 mL) and acetone (5 mL). Stirring until the solution is clear and transparent, leaving it at room temperature. Then, P3 crystals were gradually precipitated and collected as the solvent evaporated.

Synthesis of $(C_{21}H_{22}P)(Cu_2I_4)_{0.5}$ (P4). CuI (0.1 mmol), $[C_{21}H_{22}P]I$ (0.3 mmol) and H_3PO_2 (0.5

mL) were dissolved in acetonitrile (5 mL) and ethanol (5 mL). Stirring until the solution is clear and transparent, leaving it at room temperature. Then, P4 crystals were gradually precipitated and collected as the solvent evaporated.

Characterizations

The single crystal data of L1-L2 and P1-P4 were collected at 293 K using the XtaLAB AFC12 X-ray four-circle single crystal diffractometer (Rigaku) equipped with a CCD-detector using a graphite monochromator and the Cu K α radiation source. The structures were solved with the olex2 program and refined on 2F by full-matrix least-squares methods using the SHELXL program package. Powder X-ray diffraction (PXRD) patterns were taken on an Aeris PXRD diffractometer (PANalytical Corporation, the Netherlands) operating at 40 kV and 15 mA with a monochromatized Cu K α radiation ($\lambda = 1.5406 \text{ \AA}$). The photoluminescence excitation (PLE), photoluminescence (PL), PL decay spectra and photoluminescence quantum yields (PLQY) measurements were performed on a FLS1000 fluorescence spectrophotometer (Edinburgh Instruments Ltd., UK).

Calculations about temperature-dependent FWHM

The value of S is determined by fitting the FWHM at various temperatures using the following equation:

$$FWHM = 2.36\sqrt{S}\hbar\omega_{phonon} \sqrt{\coth\frac{\hbar\omega_{phonon}}{2k_B T}} \quad (1)$$

where \hbar represents the reduced Planck constant, ω_{phonon} denotes the phonon frequency, and k_B is the Boltzmann constant.

Figure Captions:

Table S1. The crystal structure parameters of L1 and L2.

Table S2. The crystal structure parameters of P1-P4.

Table S3. ICP measurements of Cu and I in P1-P4.

Figure S1. Scanning electron microscope (SEM) image and EDS mapping of Cu, Br, I and P elements for L1-L2 and P1-P4.

Figure S2. The UV-vis absorption spectra of L1-L2 and P1-P4.

Figure S3. The PLE-dependent PL spectra of L2 and P2-P4.

Figure S4. Temperature-dependent PL spectra of L2 and P2-P4.

Figure S5. Experimental and fitted temperature-dependent FWHM for L1 and L2.

Figure S6. The photos of the gradual change process for the structural transformation.

Figure S7. The PXRD patterns of L2 after treating with CH₃OH or CH₃CN compared with P3 and P4.

Table S1. The crystal structure parameters of L1 and L2.

Compound	(C ₂₁ H ₂₂ P) ₂ (CuBr ₃)·H ₂ O (L1)	(C ₂₁ H ₂₂ P) ₂ (CuI ₃)·0.62H ₂ O (L2)
Formula	C ₄₂ H ₄₆ Br ₃ CuOP ₂	C ₄₂ H _{45.25} CuI ₃ O _{0.62} P ₂
Molecular weight	932.00	1066.17
Crystal system	Monoclinic	Monoclinic
Space group	<i>Cc</i>	<i>Cc</i>
<i>a</i> (Å)	10.1684(3)	10.1359(2)
<i>b</i> (Å)	23.2010(6)	23.6427(4)
<i>c</i> (Å)	17.4735(5)	17.8625(4)
α (°)	90.00	90
β (°)	105.108(3)	102.533(2)
γ (°)	90.00	90
<i>V</i> (Å ³)	3979.81(19)	4178.57(15)
<i>Z</i>	4	4
ρ_{calc} (g/cm ³)	1.555	1.695
μ (mm ⁻¹)	3.673	2.846
F(000)	1880.0	2081.0
Reflection collected	18194	24712
Data/restraints/parameters	6397/29/448	8901/10/447
Goodness-of-fit on F ²	1.112	1.045
R [<i>I</i> >= 2 σ (<i>I</i>)]	$R_1 = 0.0450,$ $wR_2 = 0.1199$	$R_1 = 0.0283,$ $wR_2 = 0.0678$
R [all data]	$R_1 = 0.0472,$ $wR_2 = 0.1208$	$R_1 = 0.0307,$ $wR_2 = 0.0690$
$R_1 = \Sigma F_o - F_c / \Sigma F_o , wR_2 = \Sigma[w(F_o^2 - F_c^2)^2] / \Sigma[w(F_o^2)^2]^{1/2}$		

Table S2. The crystal structure parameters of P1-P4.

Compound	(C ₂₁ H ₂₂ P)(Cu ₂ I ₄) _{0.5} (P1)	(C ₂₁ H ₂₂ P)(Cu ₂ I ₄) _{0.5} (P2)	(C ₂₁ H ₂₂ P)(Cu ₂ I ₄) _{0.5} (P3)	(C ₂₁ H ₂₂ P)(Cu ₂ I ₄) _{0.5} (P4)
Formula	C ₄₂ H ₄₄ Cu ₂ I ₄ P ₂	C ₄₂ H ₄₄ Cu ₂ I ₄ P ₂	C ₄₂ H ₄₄ Cu ₂ I ₄ P ₂	C ₄₂ H ₄₄ Cu ₂ I ₄ P ₂
Molecular weight	1245.39	1245.39	1245.39	1245.39
Crystal system	Monoclinic	Monoclinic	Monoclinic	Monoclinic
Space group	<i>P</i> 2 ₁ / <i>n</i>			
<i>a</i> (Å)	11.6304(4)	11.6293(3)	11.6568(16)	11.6416(4)
<i>b</i> (Å)	12.4197(3)	12.4221(3)	12.3997(13)	12.4211(4)
<i>c</i> (Å)	15.4062(4)	15.4045(4)	15.3791(16)	15.4172(5)
<i>α</i> (°)	90	90	90	90
<i>β</i> (°)	94.555(3)	94.582(2)	94.502(11)	94.557(3)
<i>γ</i> (°)	90	90	90	90
<i>V</i> (Å ³)	2218.34(11)	2218.23(10)	2216.0(4)	2222.30(13)
<i>Z</i>	4	4	4	4
ρ_{calc} (g/cm ³)	1.864	1.865	1.866	1.861
μ (mm ⁻¹)	3.842	3.842	3.846	3.835
F(000)	1192.0	1192.0	1192.0	1192.0
Reflection collected	26570	26014	25835	26251
Data/restraints/parameters	5818/0/228	5791/0/229	5798/0/228	5835/0/228
Goodness-of-fit on F ²	1.035	1.027	1.022	1.062
R [<i>I</i> >= 2σ (<i>I</i>)]	<i>R</i> ₁ = 0.0308, <i>wR</i> ₂ = 0.0703	<i>R</i> ₁ = 0.0248, <i>wR</i> ₂ = 0.0534	<i>R</i> ₁ = 0.0332, <i>wR</i> ₂ = 0.0697	<i>R</i> ₁ = 0.0233, <i>wR</i> ₂ = 0.0638
R [all data]	<i>R</i> ₁ = 0.0449, <i>wR</i> ₂ = 0.0755	<i>R</i> ₁ = 0.0381, <i>wR</i> ₂ = 0.0570	<i>R</i> ₁ = 0.0581, <i>wR</i> ₂ = 0.0797	<i>R</i> ₁ = 0.0328, <i>wR</i> ₂ = 0.0673

$R_1 = \Sigma ||F_o| - |F_c|| / \Sigma |F_o|$, $wR_2 = \Sigma [w(F_o^2 - F_c^2)^2] / \Sigma [w(F_o^2)^2]^{1/2}$

Table S3. ICP measurements of Cu and I in P1-P4.

Samples	Cu (%)	I (%)
P1	10.76	6.13
P2	10.89	8.00
P3	10.14	9.76
P4	10.10	10.59

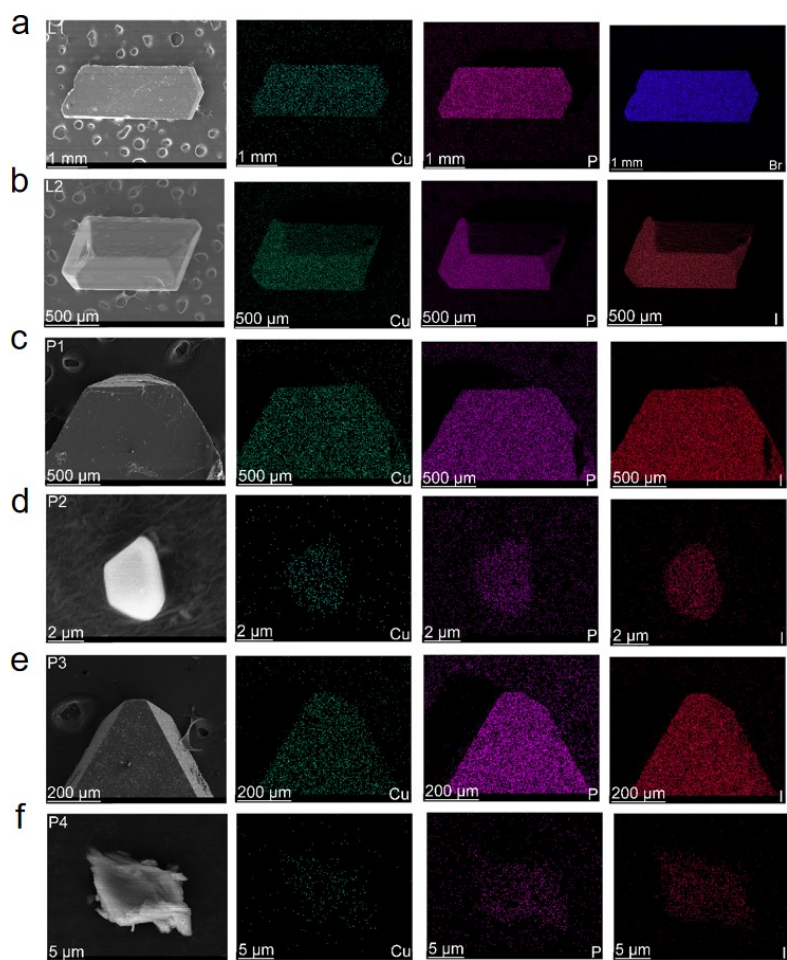


Figure S1. Scanning electron microscope (SEM) image and EDS mapping of Cu, Br, I and P elements for L1-L2 (a-b) and P1-P4 (c-f).

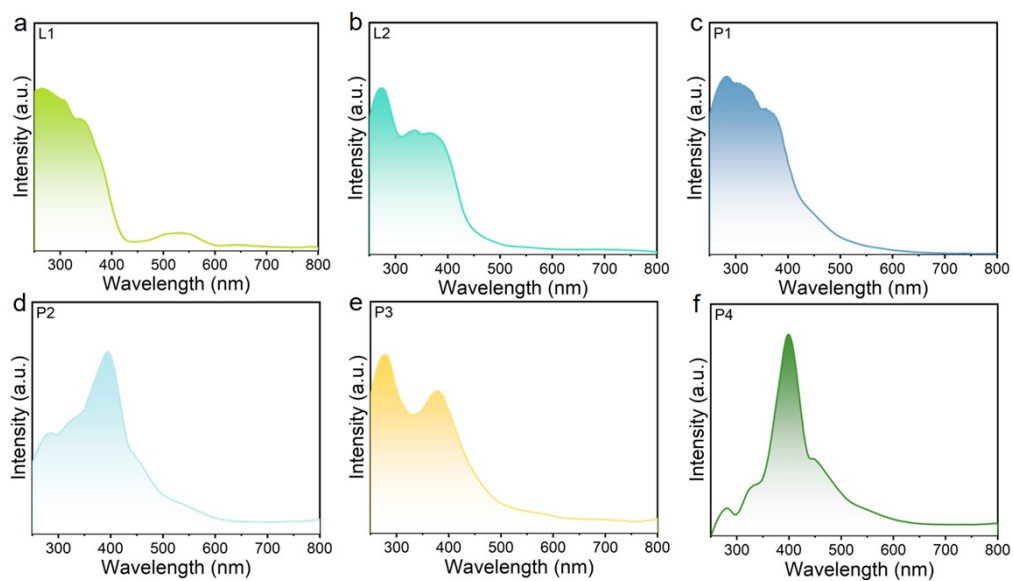


Figure S2. The UV-vis absorption spectra of L1-L2 (a-b) and P1-P4 (c-f).

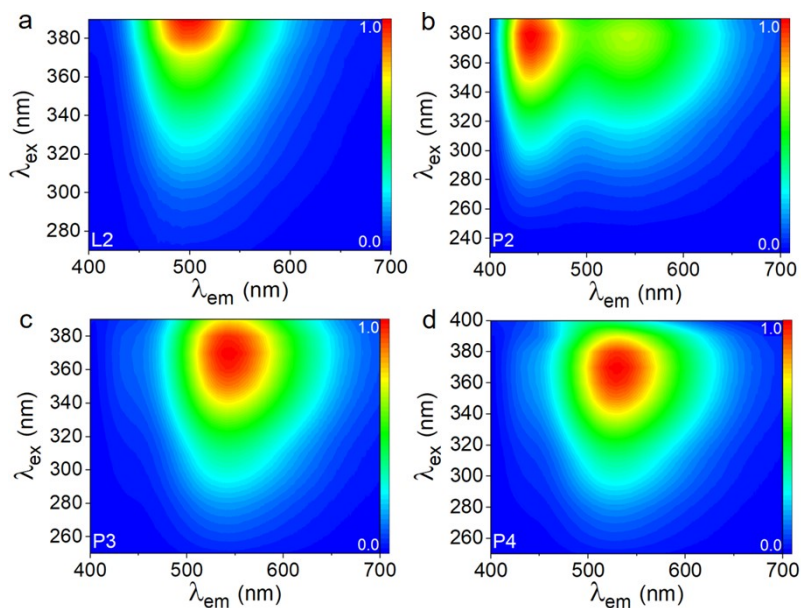


Figure S3. The PLE-dependent PL spectra of L2 (a) and P2-P4 (b-d).

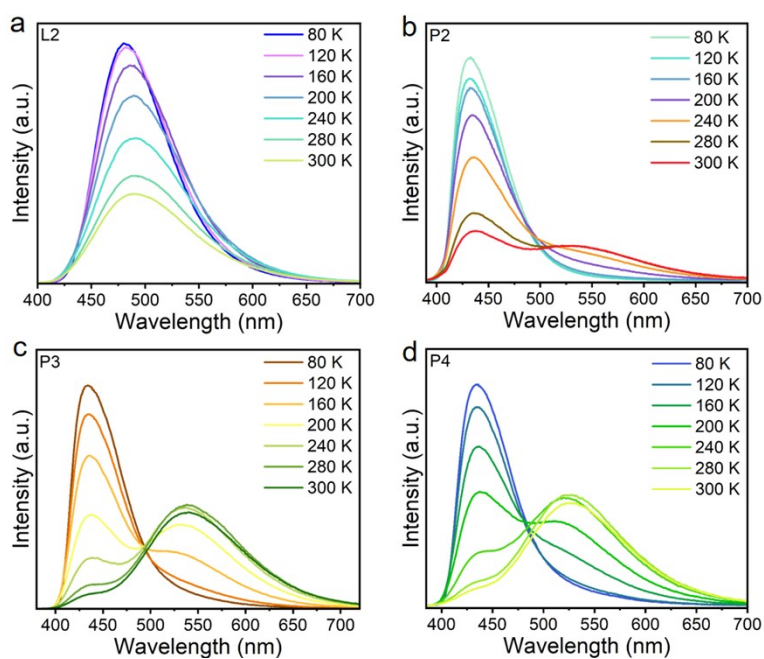


Figure S4. Temperature-dependent PL spectra of L2 (a) and P2-P4 (b-d).

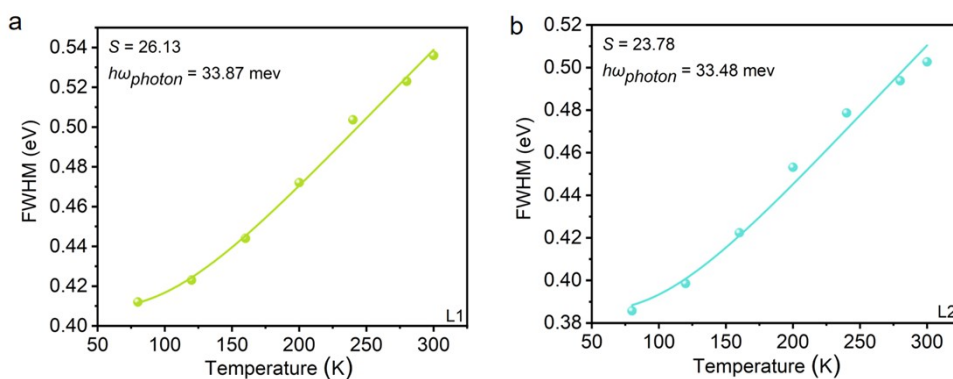


Figure S5. Experimental and fitted temperature-dependent FWHM for L1 (a) and L2 (b).

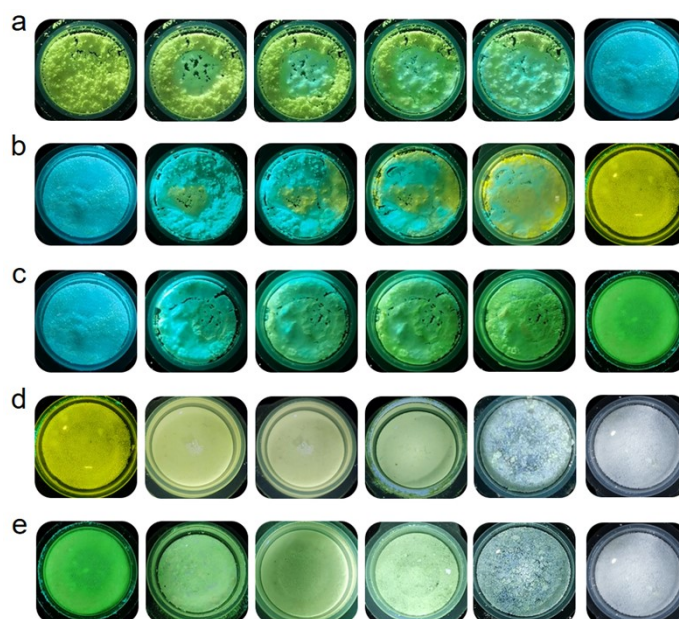


Figure S6. The photos of the gradual change process for the structural transformation from L1 to L2 (a), L2 to P3 (b), L2 to P4 (c), P3 to P2 (d), P4 to P2 (e).

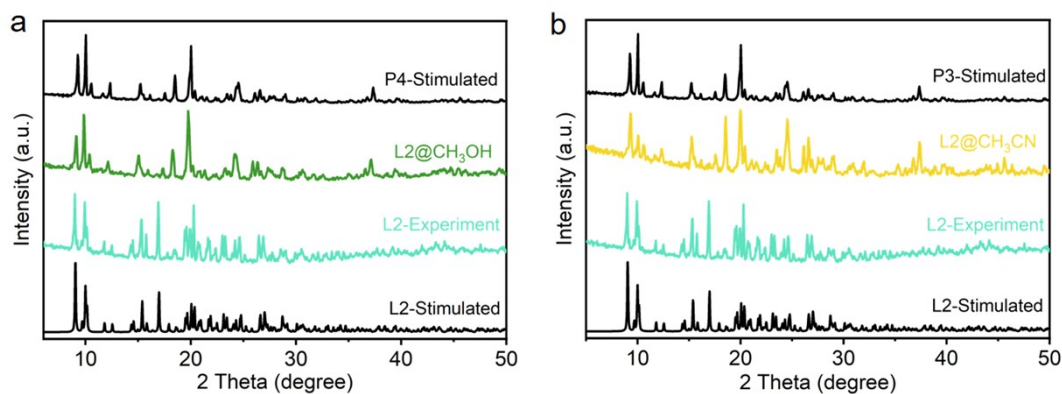


Figure S7. The PXRD patterns of L2 after treating with CH_3OH (a) or CH_3CN (b) compared with P3 and P4.